Neurocomputing 364 (2019) 239–244

Contents lists available at ScienceDirect

Neurocomputing

journal homepage: www.elsevier.com/locate/neucom

Optical neural networks based on optical fiber-communication system

Tian-You Cheng, Da-Ya Chou, Ching-Chuan Liu, Ya-Ju Chang, Chii-Chang Chen*

Department of Optics and Photonics, National Central University, Jhongli 32001, Taiwan

ARTICLE INFO

Article history:
Received 6 March 2019
Revised 3 June 2019
Accepted 17 July 2019
Available online 23 July 2019

Communicated by Dr. Vincenzo Conti

Keywords:
Neural networks
Reservoir computing
Optical fibers

ABSTRACT

In this work, we propose a novel design for optical neural network system based on reservoir computing. The optical neurons in the system consist of directional couplers, optical fibers, and optical amplifiers. The nonlinear activation function of optical neuron can be obtained by the optical amplifiers. Mach–Zehnder phase modulators and the directional couplers are used to build the readout matrix in the output layer. The performance of the system is studied by a commercial software of optical fiber telecommunication system. The results show that the randomly connected optical neuron networks of the reservoir computing can provide a better performance.

1. Introduction

Machine learning [1,2] has been an attractive technique because of raising performance with experience computed from big data. It has provided a grand playground for researchers across computer science, mathematics, material science, engineering, physics, and medicine. The application range includes the navigation on Mars [3], speech/visual recognition [4,5], consumer-targeted marketing [6], the health score of restaurant [7], the fashion suggestion [8], the prediction of the power loading of residential building [9], the rainfall forecasting [10], the prediction of the traffic flow [11], the identification of the students who need to be assisted [12] and the movies in that people may be interested [13], etc. The classification of two-dimensional images can be achieved by using convolution neural network [14]. Recently a method deepening the fully connected neural network showed that it is easier to train the data for the irregular regression and time-series forecasting [15]. A hybrid learning algorithm for multi-layer neural networks has been found to be more suitable for hardware implantation [16]. Three-dimensional information extracted from two-dimensional images for the application the human pose recovery is also started to be investigated [17]. The recovery error has been reduced by 20–25% [18].

Recurrent Neural Network (RNN) is one of the methods which are characterized by feedback ("recurrent") loops in the neuron networks. It can maintain an ongoing activation even in the absence of input and thus has a dynamic memory [19]. Owing to the integrating both the highly transformable computational capabilities and the large dynamic memory, RNN represents a very powerful generic tool. Recently, RNN has been demonstrated a great success in construction of gene regulatory network [20], and language modeling [21]. Unfortunately, the long training time and the numerous parameters to be optimized are required. This results in the fact that RNN is not suitable for the applications where the short training time is necessary.

Reservoir computing (RC) is a neuromorphic computing method in which the nonlinear response of each neuron provides the capability to classify the input data into a higher-dimensional space [22,23]. The neurons consist of a feedback loop and a nonlinear activation function. Any nonlinear activation function such as Mackey–Glass oscillator [24], sinusoidal [25], tanh [26], sigmoid [25] or chaotic functions [27] can be used for this purpose. A readout matrix in output layer is trained by using a pseudo-inverse matrix method [28] with which the time-consuming problem of RNN may be exempted.

For RC performed by the conventional personal computers, as the input and target data sizes are huge, the calculation time is mainly consumed by the multiplications between the input data and the matrix in reservoir layer. The required memory size might be huge. Some high performance CPUs or GPUs might be used to reduce the calculation time. The optical reservoir computing system has been experimentally demonstrated to be a candidate to significantly ameliorate the calculation performance [29]. To realize the optical neuron networks, the Field Programmable Gate Array (FPGA) was used due to the rapid re-programmability [28]. However, the time delay for the calculation and the limited memory size in FPGA as well as the time for the conversion between optical and electronic (O–E) signals could restrict the possibility of the

* Corresponding author.
E-mail address: trich@dop.ncu.edu.tw (C.-C. Chen).

https://doi.org/10.1016/j.neucom.2019.07.051
0925-2312/

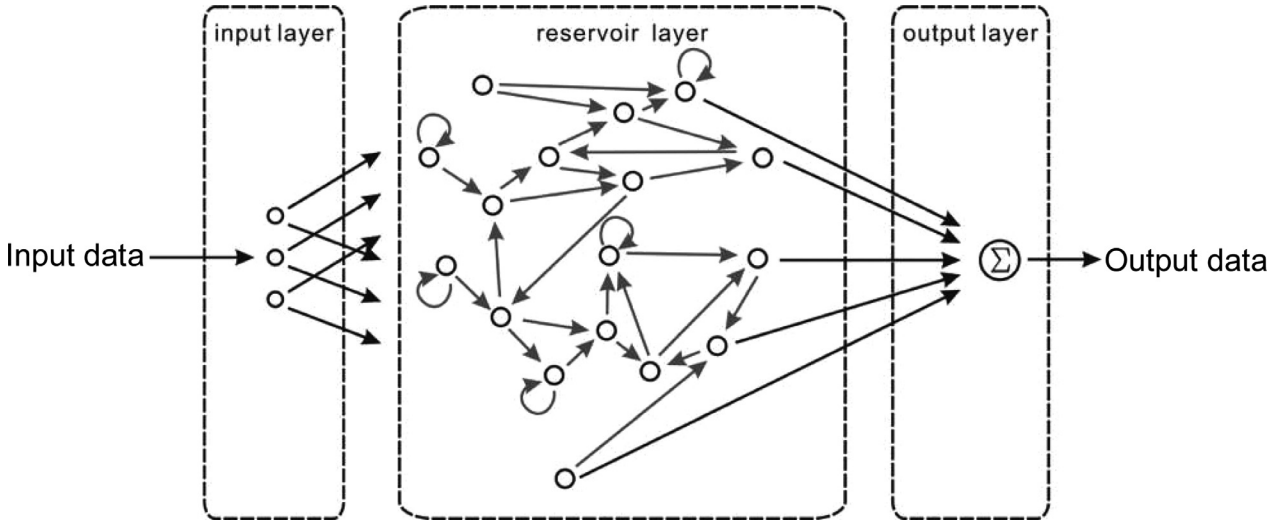

Fig. 1. Schematic of the reservoir computing system.

applications. An all-optical RC system in free-space using a spatial light modulator and a diffractive optical element has been demonstrated recently [30]. The readout matrix learning is realized in tuning the digital micro-mirror devices. The learning task can be completed after 1000 iterations.

During the last decades, optics has been proved to be the best means of conveying information from one point to another [31]. Remarkable speed and multiplexing capability of optics makes it very attractive for ultrafast data transmission, and information processing [32]. The potential role of optics in supercomputing is still under consideration. In this work, we propose a novel optical reservoir computing system. The system is composed of the input layer, the reservoir layer and the output layer. The input weight matrix for the input layer consists of the directional couplers. For the nonlinear activation function required in reservoir layer, it has been implemented using birefringent interferometer [27], $LiNbO_3$ Mach–Zehnder interferometer [33], semiconductor optical amplifiers [34], semiconductor saturable absorber mirror [35], microring [36], and ring resonators [37]. In this work, we use the all-optical loop formed by optical fibers and erbium-doped fiber amplifier (EDFA) to obtain the nonlinear activation function. No O–E conversion is required in the reservoir layer. The time consumption problem can be lessened. In literature, for the readout matrix of the output layer, a configuration with $LiNbO_3$ Mach–Zehnder intensity modulator and a balanced photodiode has been proposed [38]. In this work, a simple configuration using a Mach–Zehnder phase modulator and the directional coupler is proposed to build the readout matrix in output layer. We study the entire optical fiber-based RC system using the commercial software for optical fiber telecommunication system. In RC, it is reported that the neurons in the reservoir should be randomly connected to obtain a higher performance [26]. In this work, the performance of neuromorphic computing with and without interconnection between optical neurons is also investigated. The purpose of the system is to provide the faster calculation performance compared to modern computers. The results obtained in this study will be further used to build the miniature system with integrated optics and nano-optics components.

2. Principle of reservoir computing

The RC system is composed of the input, reservoir and output layers which consist of the input weight matrix W^{in}, the recurrent weight matrix W, and the readout matrix W^{out}, respectively. The schematic of the RC system is illustrated in Fig. 1. The input layer which corresponds to the matrix W^{in} is used to scale the size of the input data to the size of the reservoir layer which corresponds to the matrix W. The learning is completed in a single pass through training data. The optimal readout matrix W^{out} in the output layer is used to convert the result of the reservoir layer to the output of the RC system.

The RC is a recurrent system which consists of a temporal finite internal states x(n) (typically called neurons), which are perturbed by temporally external input u(n) in discrete time.

The neuron can be described as a function of the current input and its previous calculation result which can be expressed by [39]

$$\tilde{x}(n) = f\left(W^{in}[1; u(n)], Wx(n-1)\right) \tag{1}$$

$$x(n) = (1-\alpha)x(n-1) + \alpha\tilde{x}(n) \tag{2}$$

where the function f is the nonlinear activation function of the neuron. The hyperbolic tangent function, tanh(), is usually used as the nonlinear activation function to converge the output of neurons within −1 and 1. α is the leaky rate. W^{in} is the input weight matrix. W is a recurrent weight matrix of internal network connection. The network output $y(n)$ is given by

$$y(n) = W^{out}[1; u(n); x(n)] \tag{3}$$

where W^{out} is the readout matrix. By collecting the training data [1; $u(n)$; $x(n)$] and the training target signal, the readout matrix W^{out} can be obtained by the pseudo-inverse matrix method [28]. The normalized root mean square error (NRMSE) is used to estimate the difference between the theoretical output and the system output, given by

$$NRMSE = \frac{\sqrt{\frac{\sum_{i=1}^{N}(Y'-Y)^2}{N}}}{(max(Y') - min(Y'))} \tag{4}$$

where Y' and Y are the theoretical output and the output of RC, respectively. N is the number of the evaluated samples. $max(Y')$ and $min(Y')$ represent the maximum and minimum values of Y', respectively. When the output of RC is close to the theoretical output, the NRMSE approaches 0.

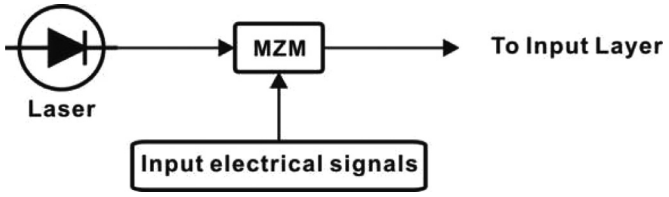

Fig. 2. Generation of input optical signals. A laser at the wavelength of 1550 nm is used as the light source. The time-dependent input electrical signals are applied to drive a Mach–Zehnder modulator thereby producing time-dependent optical signals. The optical signal is injected to the input layer.

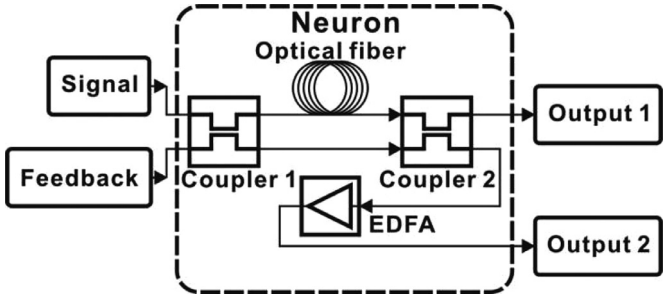

Fig. 3. Structure of optical neuron which consists of two optical couplers, an EDFA, and a 53 m-long optical fiber.

3. Optical RC system

3.1. Input optical signals

The input of the RC system is depicted in Fig. 2. A laser emitting at the wavelength of 1550 nm is chosen to serve as the light source. The 3-dB line width of the laser is 10 pm which is a typical value of 1550 nm laser source. The power of the laser is varied from 0.01 W to 10 W to investigate the performance of the RC system. Although the power of laser light above 1 W might induce the nonlinear effect in the optical fibers, in this work, we ignore the non-linear effect to investigate the feasibility of the system. The light is launched into the Mach–Zehnder modulator (MZM) on which the input electrical signals are applied to produce the modulated the optical signals. Typical Mach–Zehnder modulator is used in the simulation. The V_π is 3.11V. The bandwidth is not defined to obtain the perfect triangular and rectangular optical signals.

3.2. Optical neuron

The schematic of the optical neuron is shown in Fig. 3. It consists of optical fibers, directional couplers, and EDFA. The optical fiber is chosen to be single mode with the length of 53 m. The coupling ratio of the directional couplers is 50%. The input signal is launched into the directional coupler 1. The two outputs of the directional couplers 1 and the two inputs of the directional coupler 2 are connected directly and connected using the 53m-long optical fiber, respectively. One of the outputs of the directional coupler 2 serves as the output of the optical neuron. Another one is connected to the EDFA which provides the nonlinearity for activating the neuron. The saturation power and the small signal gain of the EDFA are chosen to be 0.1 W and 10, respectively. The noise figure of all EDFA is set to be 4 dB, a typical value of a commercial EDFA product. The output 2 of the optical neuron could be connected back to the feedback of the same optical neuron or to feedback the other optical neurons. Therefore, the recurrence of signals and the interconnection between the optical neurons can be achieved.

3.3. RC systems without and with interconnection between optical neurons

Two types of RC systems which consist of two optical neurons are depicted in Fig. 4. The input optical signals are launched into the input layer which consists of a directional coupler acting as the input weight matrix W^{in}. For the reservoir computing, the elements of W^{in} are defined randomly between 0 and 1. For the corresponding components in our optical RC system, directional couplers, the coupling ratio is defined randomly to be 0.55. The reservoir layer W consists of two optical neurons. Fig. 4(a) shows the RC system without interconnection between optical neurons. Each optical neuron's output 2 signals are fed into its own feedback [blue dashed line in Fig. 4(a)]. The RC system with interconnection between optical neurons is depicted in Fig. 4(b). [red dashed line in Fig. 4(b)]. Each neuron's output 2 is fed into the other neuron's feedback. The multiplication between the output signals of the optical neurons and the readout matrix W^{out} can be approximately achieved using the directional coupler in the output layer. To perform the learning process, the pseudo-inversion of the readout matrix is replaced by the optical delay tuning of the phase modulator in the output layer to optimize the output data with the lowest NRMSE. The coupling ratio of the directional coupler is chosen to be 50% to obtain the higher visibility of the optical interference. The optical signals are converted to the electrical signals by the photodetector. The quantum efficiency of the photodetector is set to be 80% which is typical value of the commercial components.

4. Results and discussion

To evaluate the performance of the RC systems without and with interconnection between optical neurons, the input signal, which is composed of randomly arranged rectangular and triangular waveforms, is launched into the RC system as shown in Fig. 5(a). The input optical signals are modulated between 0 and 0.1 W. The corresponding theoretical outputs of the RC system are 1 (high-level output) and 0 (low-level output) for the rectangular and triangular waveforms, respectively, as shown the red line in Fig. 5(a).

The RC systems is simulated by the commercial software for optical-fiber telecommunication system, OptSim. The optical delay is tuned using the phase modulator (PM) between one of the optical neurons and the directional couplers in the output layer to obtain the lowest NRMSE. Fig. 5(b) and (c) shows the simulation results of the RC systems without and with interconnection between optical neurons, respectively. Black and red lines represent the output signals of the RC system and the theoretical output signals, respectively. We can observe that the high-level and low-level outputs can be obtained when the input optical signals are rectangular and triangular waveforms, respectively. The result shows that the RC system can classify the waveforms of the input optical signals.

To evaluate the NRMSE of the RC system, the max(Y') and min(Y') in Eq. (4) are calculated by averaging the power of the signals for high-level and low-level output. The NRMSE for Fig. 5(b) and (c) are 0.19 and 0.14, respectively. It is found that the NRMSE of the RC system with interconnection between optical neurons is lower than that without interconnection between optical neurons. The result is consistent with the property of RC method in which the neurons in the reservoir should be randomly connected [26].

4.1. Performance of RC system for linear and nonlinear operation in EDFA

According to the property of RC method, the neuron should be activated by a nonlinear activation function [39]. Under this

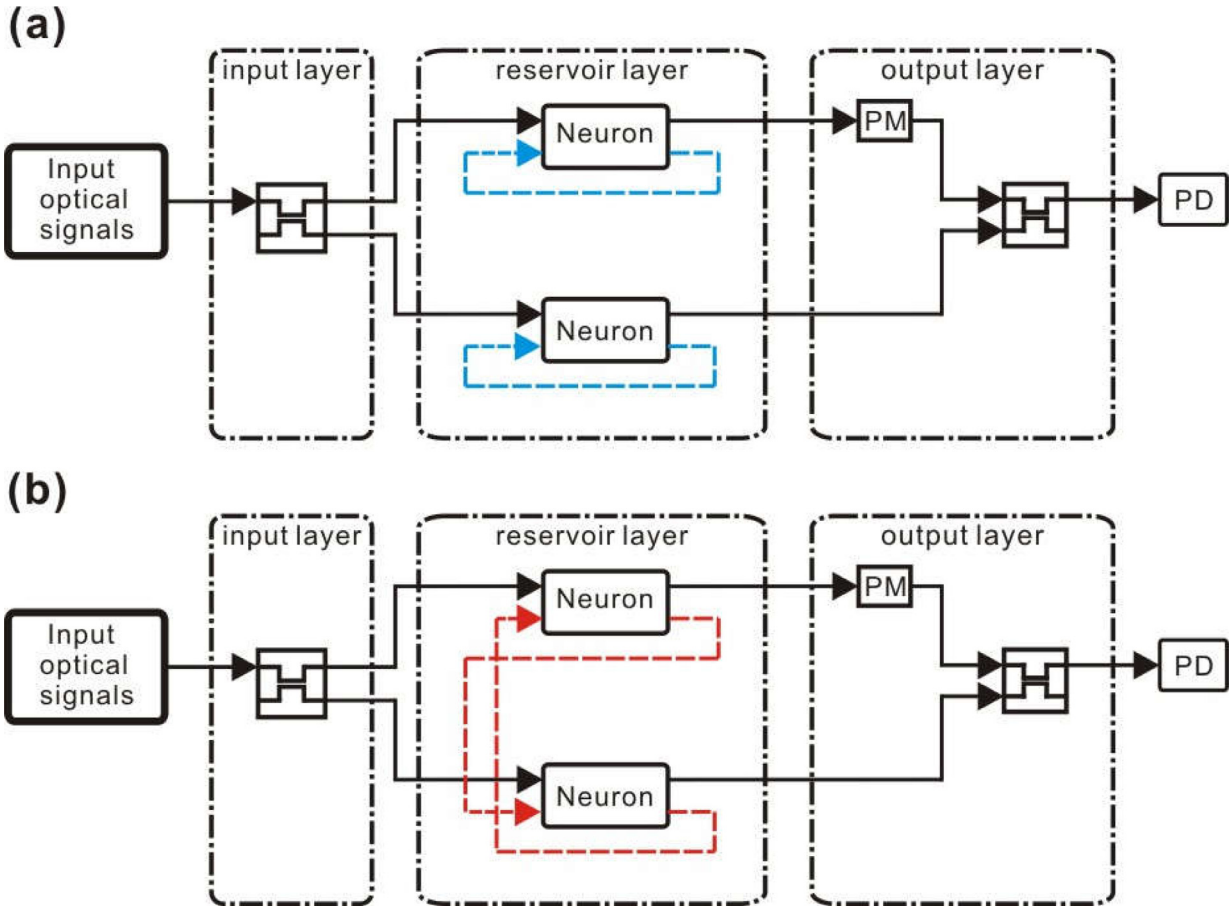

Fig. 4. RC systems (a) without and (b) with interconnection between optical neurons. PM and PD stand for the phase modulator and the photodetector, respectively. The blue dashed line indicates the fact that the output 2 of the optical neuron is fed into the feedback of the same optical neuron. There is no interconnection between optical neurons. The red dashed line indicated the fact that the output 2 of the optical neuron is fed into the feedback of the other optical neuron. There is an interconnection between the two optical neurons.

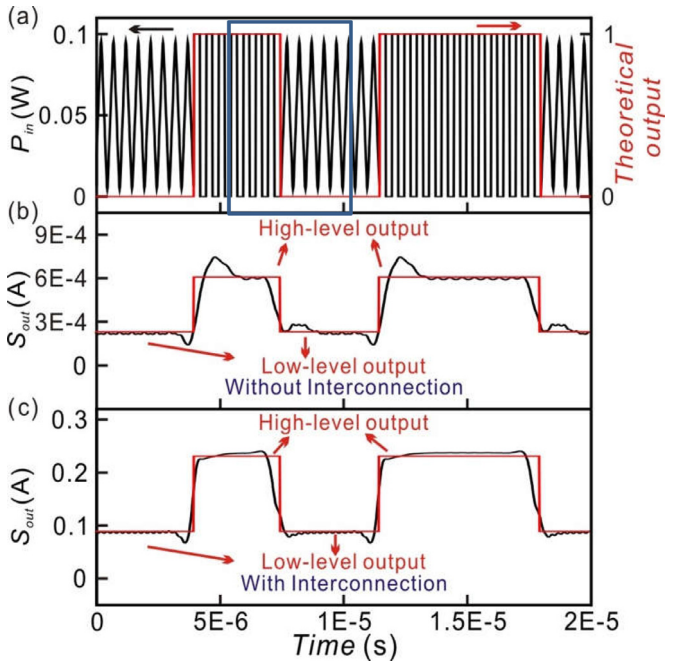

Fig. 5. (a) Input optical signals (black line) and theoretical output (red line) of RC system. (b) and (c) represent the output signals of RC system without and with interconnection between the optical neurons, respectively.

nonlinear condition, the optical neuron can provide the capability to classify the input data into a higher-dimensional space [22]. In this study, the nonlinear activation function is provided by the EDFA in the optical neurons. According to the gain model of EDFA in our simulation, the gain coefficient G is expressed as

$$G = \frac{G_0}{1 + G_0 \frac{P_{in}}{P_{sat}}} \tag{5}$$

where G_0 is the small signal gain. P_{sat} is the saturation output power. P_{in} is the input power. P_{sat} and G_0 of EDFA are chosen to be 0.1 W and 10, respectively. Fig. 6 shows the output power of EDFA in varying the input power P_{in} from 0.01 W to 10 W. When the input power of EDFA is lower than 0.05 W, G is approximately constant leading to the fact that the relation between the input and output power of the EDFA is approximately linear. When the input power increases from 0.05 W, the output power bends over where the EDFA operates in the nonlinear regime.

To study the performance of the RC system for linear and nonlinear operation in EDFA, the power of the input optical signals of the RC system is varied from 0.01 W to 10 W. Fig. 7 shows the simulation results of RC system with interconnection between optical neurons. Fig. 7(a) shows the output signals of RC system when the power of the input optical signal is 0.01 W. In this case, the EDFA in the optical neurons is operated in the linear regime. The corresponding NRMSE of the RC system is 0.48. Fig. 7(b) and (c) shows the output signals of RC system when the power of the input optical signal is 1 W and 10 W, respectively. The results show

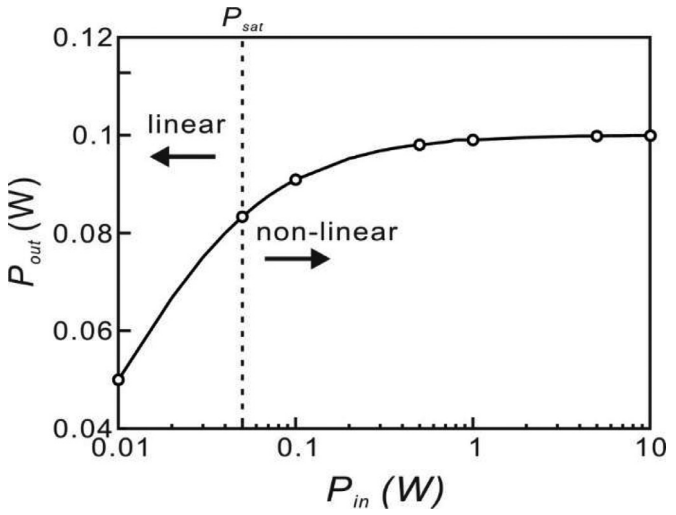

Fig. 6. Output power of the EDFA as the input power is varied from 0 to 10 W. ($P_{sat} = 0.1$ W, $G_0 = 10$). The dashed line indicates the fact that when the input power is lower than 0.05 W, the EDFA is approximately operated in the linear regime. When the input power is larger than 0.05 W, the EDFA is operated in the non-linear regime.

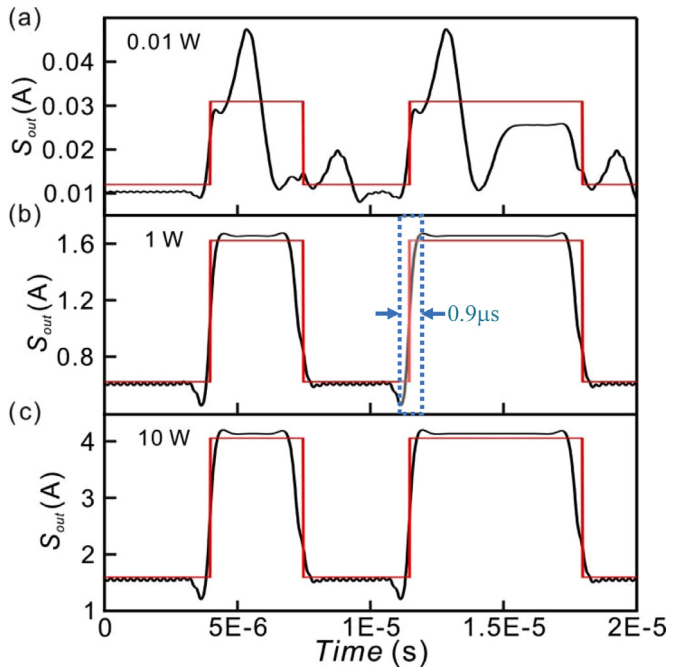

Fig. 7. Outputs of the RC system with interconnection between optical neurons under the difference power of the input optical signals. From top to bottom: power of the input optical signals is (a) 0.01 W (b) 1 W (c) 10 W, respectively. The red line indicates the theoretical output.

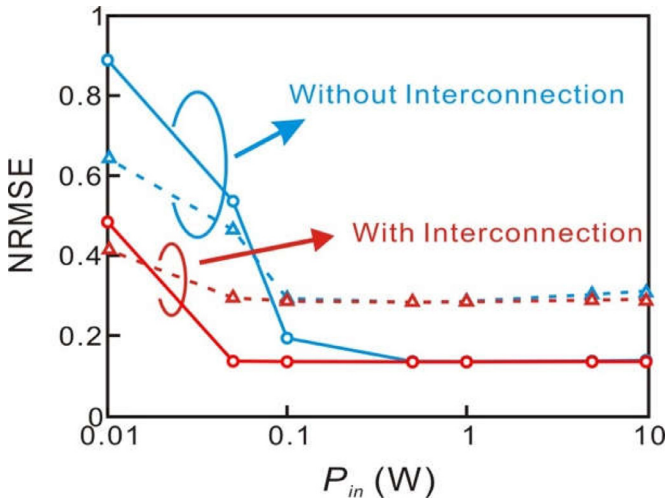

Fig. 8. NRMSE versus power of the input optical signals. Solid lines represent the NRMSE obtained by defining min(Y') to be the average of low-level output signals. Dashed lines represent the NRMSE obtained by defining min(Y') to be 0. Blue (red) lines indicate the RC systems without (with) interconnection between optical neurons.

that the output signals (black lines) are close to theoretical output (red lines). The NRMSE for Fig. 7(b) and (c) are 0.133 and 0.134, respectively. These results demonstrate the property of RC method in which optical neurons should be activated by a nonlinear activation function [39].

The correlation between NRMSE and the power of the input optical signals are depicted in Fig. 8. The power of the input optical signals of the RC systems without and with interconnection between neurons is varied from 0.01 W to 10 W. When the power of the input optical signals is increasing from 0.01 W to 0.1 W where the EDFA is checked to operate in the linear regime, the NRMSE decreases. The NRMSE of the RC systems without and with interconnection between optical neurons decreases from 0.89 to 0.19 (blue solid line) and 0.48 to 0.139 (red solid line), respectively. As the operation power is above 0.1 W where the EDFA is operating in the non-linear regime, the NRMSE reaches the minimum. The NRMSE of the RC systems without and with interconnection between optical neurons are 0.134 and 0.133, respectively. As the power of the input optical signals is higher than 1 W, the NRMSE is almost constant where the EDFA is operating in the saturated regime. The results show the fact that the non-linear function of the neurons is required to obtain the capability of the signal recognition in the optical RC system. This result shows that we can obtain the low NRMSE with the optical input power of 0.05 W in the system with the interconnection between neurons indicating that the nonlinear effect of optical fiber (or waveguide) might not be significant in the further development of the miniature system with integrated optics or nano-optics components.

In Fig. 7(b), we show the rising time of the output signal is around 0.9 μs which corresponds to the longest calculation time. The minimum calculation time of the optical RC system corresponds to the delay of the 53 m-long optical fiber in the neurons to be 0.27 μs. We compare with the RC program using Matlab 2019a in a personal computer with 3.6 GHz CPU (Intel core i7-4790). The size of $\boldsymbol{W}$ of Eq. (1) is set to be 10×10. The input signals are triangular and rectangular waves as those of the optical RC system used in this study. The longest and shortest time and the mean time to obtain each network output $y(n)$ using Matlab and Eqs. (1)–(3) is 464 μs, 0.9 μs and 1.6 μs, respectively. The present study has shown a shorter calculation time for the optical RC system than personal computer. In this study, the period of each triangular or rectangular signals is modulated to be 0.5μs corresponding to the bit rate of 2 GHz. By using the modern $LiNbO_3$ modulator and detector of 40 GHz, the performance of the optical RC system could be significantly enhanced.

5. Conclusion

We have proposed an all-optical reservoir computing system based on optical fiber-based system. The optical neuron in reservoir consists of optical fibers, directional couplers, and an erbium-doped optical fiber amplifier. The NRMSE of the RC system with interconnection between optical neurons is lower than that without interconnection between optical neurons. The fact that the optical

neurons in the reservoir should be randomly connected and the optical neurons should be activated by a nonlinear activation function have been demonstrated. The components simulated in this study could be further replaced by the integrated optics or nano-optics components. The lowest NRMSE is obtained as the optical input power lower than 1 W. This indicates that nonlinear effect of optical fiber or waveguide in the development of the miniature system using the integrated optics and nano-optics might be avoided. The size and the power consumption of the system could be significantly reduced.

Author agreement/declaration

All authors have seen and approved the final version of the manuscript being submitted. We warrant that the article is the authors' original work, has not received prior publication and is not under consideration for publication elsewhere.

Funding source declaration

There are no funding or research grants for this work.

Permission note

All material used in the manuscript such as figures are original content.

Declaration of Competing Interest

There is no financial/personal interest.

CRediT authorship contribution statement

Tian-You Cheng: Formal analysis, Visualization, Writing - original draft. **Da-Ya Chou:** Formal analysis, Software. **Ching-Chuan Liu:** Formal analysis, Software, Visualization. **Ya-Ju Chang:** Data curation. **Chii-Chang Chen:** Conceptualization, Formal analysis, Funding acquisition, Validation, Writing - review & editing.

Acknowledgments

The author thanks Prof. Laurent Larger (FEMTO-ST/Optics Department, UMR CNRS 6174, University of Franche-Comté, 16 Route de Gray, 25030 Besançon Cedex, France) for kind tutorial and discussion.

References

[1] Y.S. Abu-Mostafa, M. Magdon-Ismail, H.-.T. Lin, Learning from Data, 1st ed., AMLBook, 2012.
[2] C.M. Bishop, Pattern Recognition and Machine Learning, Springer Science+Business Media, 2006.
[3] R. Castaño, M. Judd, R.C. Anderson, T. Estlin, Machine learning challenges in mars rover traverse science, in: Proceedings of the 2003 ICML Workshop on Machine Learning Technologies for Autonomous Space, 2003.
[4] G Hinton, et al., Deep neural networks for acoustic modeling in speech Recognition: the shared views of four research groups, IEEE Signal Process. Mag. 29 (2012) 82–97.
[5] I. Laptev, M. Marszałek, C. Schmid, B. Rozenfeld, Learning realistic human actions from movies, in: Proceedings of the 2008 IEEE Conference on Computer Vision and Pattern Recognition, 2008.
[6] C. Apte, B. Dietrich, M Fleming, Business leadership through analytics, IBM J. Res. Dev. 56 (2012) 7:1–7:5.
[7] A. Sadilek, S. Brennan, H. Kautz, V. Silenzio, nEmesis: which restaurants should you avoid today? in: Proceedings of the First AAAI Conference on Human Computation and Crowdsourcing (HCOMP-13), 2013.
[8] Z.-.L. Sun, T.-.M. Choi, K.-.F. Au, Y. Yu, Sales forecasting using extreme learning machine with applications in fashion retailing, Decis. Support Syst. 46 (2008) 411–419.
[9] A. Tsanas, A. Xifara, Accurate quantitative estimation of energy performance of residential buildings using statistical machine learning tools, Energy Build 49 (2012) 560–567.
[10] W.-.C. Hong, Rainfall forecasting by technological machine learning models, Appl. Math. Comput. 200 (2008) 41–57.
[11] Y. Lv, et al., Traffic flow prediction with big Data: a deep learning approach, IEEE Trans. Intell. Transp. Syst. 16 (2015) 865–873.
[12] A. Ahadi, R. Lister, H. Haapala, A. Vihavainen, Exploring machine learning methods to automatically identify students in need of assistance, in: ICER '15 Proceedings of the Eleventh annual International Conference on International Computing Education Research, 2015.
[13] J. Sill, Recommend a movie, win a million bucks, Eng. Sci. 73 (2010) 32–39.
[14] J. Ou, Y. Li, Vector-kernel convolutional neural networks, Neurocomputing 330 (2019) 253–258.
[15] A. Liu, Y. Laili, Balance gate controlled deep neural network, Neurocomputing 320 (2018) 183–194.
[16] S.P. Adhikari, C. Yang, K. Slot, M. Strzelecki, H. Kim, Hybrid no-propagation learning for multilayer neural networks, Neurocomputing 321 (2018) 28–35.
[17] C. Hong, J. Yu, J. Wan, D. Tao, M. Wang, Image-Based three-dimensional human pose recovery by multiview locality-sensitive sparse retrieval, IEEE Trans. Ind. Electron. 62 (2015) 3742–3751.
[18] C. Hong, J. Yu, J. Wan, D. Tao, M. Wang, Multimodal deep autoencoder for human pose recovery, IEEE Trans. Image Process. 24 (2015) 5659–5670.
[19] L. Medsker, L.C. Jain, Recurrent Neural Networks: Design and Applications, CRC Press, 1999.
[20] A. Khan, S. Mandal, R.K. Pal, G. Saha, Construction of gene regulatory networks using recurrent neural networks and swarm intelligence, Scientifica (Cairo) 2016 (2016) 1060843.
[21] W. De Mulder, S. Bethard, M.-.F. Moens, A survey on the application of recurrent neural networks to statistical language modeling, Comput. Speech Lang. 30 (2015) 61–98.
[22] L Appeltant, et al., Information processing using a single dynamical node as complex system, Nat. Commun. 2 (2011) 468.
[23] H. Jaeger, H. Haas, Harnessing nonlinearity: predicting chaotic systems and saving energy in wireless communication, Science 304 (2004) 78–80.
[24] L. Appeltant, G. Van der Sande, J. Danckaert, I. Fischer, Constructing optimized binary masks for reservoir computing with delay systems, Sci. Rep. 4 (2014) 3629.
[25] Y Paquot, et al., Optoelectronic reservoir computing, Sci. Rep. 2 (2012) 287.
[26] M. Lukoševičius, H Jaeger, Reservoir computing approaches to recurrent neural network training, Comput. Sci. Rev. 3 (2009) 127–149.
[27] R Martinenghi, et al., Photonic nonlinear transient computing with multiple-delay wavelength dynamics, Phys. Rev. Lett. 108 (2012) 244101.
[28] A. Ben-Israel, T.N.E. Greville, Generalized Inverses: Theory and Applications, 2nd ed., Springer, 2003.
[29] D. Brunner, B. Penkovsky, B.A. Marquez, M. Jacquot, I. Fischer, L. Larger, Tutorial: photonic neural networks in delay systems, J. Appl. Phys. 124 (2018) 152004.
[30] J. Bueno, S. Maktoobi, L. Froehly, I. Fischer, M. Jacquot, L. Larger, D. Brunner, Reinforcement learning in a large-scale photonic recurrent neural network, Optica 5 (2018) 756–760.
[31] G. Keiser, Optical Fiber Communications, John Wiley & Sons, 2003.
[32] B. Javidi, J.L. Horner, Real-Time Optical Information Processing, Academic Press, 2012.
[33] C.-.C Chen, et al., Phrase correction by laser ablation of a polarization independent $LiNbO_3$ Mach–Zehnder modulator, IEEE Photon. Technol. Lett. 9 (1997) 1361–1363.
[34] F Duport, et al., All-optical reservoir computing, Opt. Express 20 (2012) 22783–22795.
[35] A Dejonckheere, et al., All-optical reservoir computer based on saturation of absorption, Opt. Express 22 (2014) 10868–10881.
[36] H Zhang, et al., Integrated photonic reservoir computing based on hierarchical time-multiplexing structure, Opt. Express 22 (2014) 31356–31370.
[37] D.-.P Cai, et al., High Q-factor microring resonator wrapped by the curved waveguide, Sci. Rep. 5 (2015) 10078.
[38] A Smerieri, et al., Analog readout for optical reservoir computers, in: Proceedings of the Advances in Neural Information Processing Systems 25 (NIPS 2012), 2012.
[39] M. Lukoševičius, H. Jaeger, B. Schrauwen, Reservoir computing trends, Künstl. Intell. 26 (2012) 365–371.